Metabolomics Study of Browning Mechanism in Eggplant Fruits

Xiaohui Liu
Shanghai Academy of Agricultural Sciences https://orcid.org/0000-0002-7413-0436
Shengmei Zhang
Shanghai Academy of Agricultural Sciences
Jing Shang
Shanghai Academy of Agricultual Sciences
Aidong Zhang
Shanghai Academy of Agricultural Sciences
Zongwen Zhu
Shanghai Academy of Agricultural Sciences
Xuexia Wu (wuxuexiarose@sohu.com)
Shanghai Academy of Agricultural Sciences
Dingshi Zha
Shanghai Academy of Agricultual Sciences

Research article

Keywords: Eggplant (Solanum melongena L.), Browning, LC-MS, Metabolomics, Differential metabolites, Metabolic pathways

Posted Date: November 25th, 2019

DOI: https://doi.org/10.21203/rs.2.17727/v1

Abstract

Background: Fresh-cut fruits and vegetables is a emerging type of fruits and vegetables processing products for consumers to eat immediately or for the catering industry. Enzymatic browning is one of the crucial problems compromising the flavor and texture of fresh-cut fruit and vegetables. Eggplant is a common vegetable, which is favored by consumers. Accordingly, we used an untargeted metabolomics approach based on liquid chromatography-mass spectrometry (LC-MS) to explore the browning mechanism in peeled eggplant (Solanum melongena L .).

Results: Metabolomics revealed several hundred differential metabolites, including lipids, phenols, sugars and fatty acids. The content of these metabolites changed dynamically as the peeled time increased. The content of polyphenols, especially chlorogenic acid, increased significantly, suggesting that the main substrate for enzymatic browning in eggplant is chlorogenic acid. Furthermore, all the differential metabolite were mapped to KEGG pathway, revealing significant differences in linoleic acid metabolism, tyrosine metabolism glutathione metabolism, pentose phosphate pathway, tropane, piperidine and pyridine alkaloid biosynthesis, phenylpropanol metabolism and glycosylphosphatidylinositol(GPI)-anchor biosynthesis over time. Therefore, we speculate that some metabolic pathways that are closely connected with respiration, glycolysis, ATP synthesis, and phenolic synthesi are disturbed after peeling, under the action of enzymes, eventually leading to browning.

Conclusions: We established an untargeted metabolomics method based on LC-MS technology to explain the mechanism of eggplant browning, which may lay the foundation for better understanding the mechanism of browning during the fruits and vegetables deeply processing, and furnish new ideas and perspectives for understanding fruit and vegetable browning in the future.

Background

Metabonomics was first proposed by Nicholson et al.[1] in 1999 and interpreted to the quantitative analysis of metabolic response of an organism subjected to pathophysiological stimulation or genetic changes. Fiehn [2] proposed in 2002 that metabolomics is a qualitative and quantitative analysis method for total metabolites in the body of an organism. Metabolomics is a burgeoning omics technology, after genomics and proteomics, which can be divided into target analysis, metabolic profiling, and fingerprint analysis, based on the scope of the study objectives and metabolic coverage. These four levels can be divided into target metabolomics and non-target metabolomics. Metabolomics is widely used in drug screening and toxicity evaluation, drug quality control, clinical marker discovery, early diagnosis, therapeutic function genomics, plant breeding, microbial engineering, nutrition, environmental toxicology and other research fields [3]. A variety of metabolites, such as organic acids, sugars, lipids, amino acids and secondary metabolites as alkaloids, flavonoids, terpenes, can be monitored by qualitative analysis of metabolites based on gas chromatography or liquid chromatography in conjunction with mass spectrometry [4]. With the deepening of plant metabolomics research, we have a better understanding of plant growth regulation, development and metabolic processes and molecular mechanisms of stress response. As well as, plant metabolomics has become a forceful tool for probing physiology and biology all aspects of plant [5]. There are many factors that may affect the metabolic capacity of plant defenses such as the interaction between biological and abiotic stresses. In the study of metabolomics of sorghum root under nitrogen stress demonstrated the biosynthetic capacity of salicylic acid was impaired [6]. In the experiment of different germination capacity of pollen grains of two clones of Chinese fir (Cunninghamia lanceolata (Lamb) Hook) using metabolomics method, it was revealed that in the expression of metabolites across and between clones at all germination stages had significant differences, enriched in 14 metabolic pathways, including flavonoid and flavonol biosynthetic pathways, protein biosynthetic pathways and glycerophospholipid metabolism [7]. In order to explore the mechanism of climate and development regulating the

metabolism and antioxidant system of date palm leaves, Du et al. [8] used the non-targeted metabolomics method based on LC-MS to find that young leaves may be more responsive to the environmental change.

Solanum melongena L., commonly known as eggplant, belongs to solanaceae plants, is one of the largest genus of solanaceae plants, there are more than 1550 species. It is a common vegetable, rich in polyphenols, dietary fiber, vitamins and other nutrients, and provides a variety of health benefits such as lowering blood lipids, protecting the liver and as an antioxidant, so it is favored by consumers [9]. However, browning of eggplant occurs easily after peeling, which affects its sensory quality and nutritional value, leading to a decline in edibility and commodity. It is well known that the main factors affecting the browning of fruits are water loss on the fruit surface, biomolecular oxidation, electrolyte leakage and anthocyanin degradation [10]. Browning is caused by the destruction of cell structure during the peeling process, resulting in the release of PPO and phenolic substrates. With the occurrence of enzymatic reactions, phenols are catalyzed into quinones and finally polymerizated into brown or black substances. These substances accumulate on the surface of the slices, compromising the flavor of fresh-cut fruits and vegetables [11].

In this study, we selected 24 eggplant samples, which were divided into three groups for metabolic analysis. Eight biological replicates were made for each group. An untargeted metabolomics method based on LC-MS technology combined with qualitative analysis, multivariate statistical analysis and metabolic pathway analysis in differential metabolites was used to explore the browning mechanism in eggplant, so as to offer a feasible theoretical foundation for the processing and production of fresh-cut fruit and vegetable, and provide a reference for further investigation into the restrain of browning in other fresh-cut products.

Results

Base peak ion current check

We firstly conducted a visual inspection of the base peak ion current of all samples and found that signal peak capacity and retention time repeatability were good in all samples. Figures 1 and 2 showed the base peak chromatogram of the quality control samples in TIC+ and TIC- mode, respectively.

Establish a data matrix

Metabolomics analysis was performed using the pulp of peeled eggplant after 0 (CK), 3 and 5 min. To carry out pattern recognition, the raw data were preprocessed by the metabolomics processing software progenesis QI, including peak recognition, peak alignment, integration, baseline filtering, retention time correction, normalization. In the end, a data matrix was constructed, which include the sample name, mass-to-charge ratio (m/z), retention time (RT), ion model, and metabolites. There are 15133 m/z features in this matrix, including 7038 m/z in TIC+ and 8095 m/z in TIC- (Additional file 1: Table S1). This matrix was gone to the subsequent analysis.

Multivariate analysis

In the data matrix, the data were disposed by multivariate analysis tools (PCA, PLS-DA and OPLS-DA). PCA, PLS-DA and OPLS-DA scoring plots and validation plots of the OPLS-DA models were built for the three contrastive groups: 3min/CK, 5min/CK and 3min/5min (Fig. 3). Table 1 showed all the parameters of these models. A confidence interval is a measure of confidence, usually the bigger the better. R2X represents the cumulative interpretation rate of the multivariate statistical analysis modeling, which generally requires R2X > 0.4, indicating that the model is credible. R2 and Q2 are the parameters of response sequencing test, used to measure whether the model is overfitted. External validation generally requires Q2 < 0 to avoid over-fitting. Internal validation generally requires R2, > 0.5; The closer R2 is

to 1, the better the model. In our results, all values for Hotelling's T2 were 95% , Q2 were < 0 (Q2 = −0.849 to −0.741), R2X were >0.4, and R2 were > 0.5, indicating that the model is reliable.

Differential metabolites

According to the VIP > 1 for the first principal component in the OPLS-DA, and p-value < 0.05 were the criteria for screening differential metabolites, we identified the differential metabolites among the three contrastive groups (Additional file 2: Table S2). 256 differential metabolites were detected in the 3min/CK comparative group, 357 in the 5min/CK comparative group and 333 in the 3min/5min comparative group. Among these metabolites, 49 were common to all three groups and 119 were common between 3min/CK and 5min/CK. However, 253 metabolites were the non-repeated differential metabolites between any two groups; 114, 58 and 81 metabolites were exclusive to the 3min/CK, 5 min/CK and 3min/5min comparative groups, respectively (Fig. 4).

The 119 common differential metabolites from the 3min/CK and 5min/CK groups were further divided into three sorts represented by A, B and C, as indicated in Additional File 3: Table S3 based on STC. Furthermore, the metabolites in these three categories were grouped into eight types of compounds (Table 2). The relative expression of 33 metabolites selected from the three categories (A, B, C) is shown in the heatmap (Fig.5).

Category A included 68 metabolites. These were mainly lipids, fatty acid and carbohydrates (Table 2). The contents and expression levels of these metabolites are increased gradually. The metabolites of category B comprised 40 compounds, most of which were fatty acids and lipids (Table 2). The contents and expression levels of these metabolites decreased with increase of the peeled time. There were 11 components in category C, mainly lipids (Table 2). Interestingly, their contents and expression levels decreased at 3 min, but are increased at 5 min. However, they were lower than those at 0 min (CK) as a whole.

Metabolite content changes

Eight phenols associated with browning were selected from the data matrix. The content levels of the selected metabolites at different treatment intervals shown in Fig. 6. The contents of chlorogenic acid and E-10-Hydroxyamitriptyline increased significantly with longer time from peeling. By contrast, octyl 4-methoxycinnamic acid, trimethobenzamide, (S)-[8]-Gingerol and cis-[8]-Shogaol contents decreased significantly. However, there was no remarkable alteration in the content of some metabolites , such as ethylvanillin glucoside and glucocaffeic acid. Furthermore, the changes in the contents of the selected metabolites (Fig. 6) were similar to the expression level changes shown in the heatmap (Fig. 5).

KEGG pathway analysis.

The metabolites in categories A, B and C were mapped, respectively, using the KEGG database onto the KEGG pathways with the following results (Fig. 7).

The metabolites of category A were mainly enriched in 18 metabolic pathways: Linoleic acid metabolism, Pentose phosphate pathway, Nitrogen metabolism, Glycosylphosphatidylinositol (GPI)-anchor biosynthesis, Autophagy-other, Taurine and hypotaurine metabolism, Galactose metabolism, Aminoacyl-tRNA biosynthesis, Arginine biosynthesis, Arginine and proline metabolism, Alanine, aspartate and glutamate metabolism, C5-Branched dibasic acid metabolism, Glutathione metabolism, Butanoate metabolism, Histidine metabolism, ABC transporters, Glyoxylate and dicarboxylate metabolism, and Glycerophospholipid metabolism. Of these, Glycosylphosphatidylinositol (GPI)-anchor biosynthesis, Linoleic acid metabolism, Autophagy-other and Nitrogen metabolism showed extremely significant differences in the 3min/CK and 5min/CK two comparative groups at the p < 0.01 level of significance, while the others revealed a

significant difference ($p < 0.05$). There was a remarkable difference ($p < 0.05$) in the metabolites of category B that were only enriched in one metabolic pathway, Tropane, piperidine and pyridine alkaloid biosynthesis. Finally, the metabolites of category C were enriched in Tyrosine metabolism and had a remarkable difference ($p < 0.05$) similarly.

Discussion

Metabolomics is a part of systems biology and can uncover relationships between metabolites and physiology/pathology by qualitative or quantitative analysis of metabolites. Enzymatic browning of fruits is an extremely complex process. Phenols, as important substrates of enzymes, play a key role in the browning that occurred during the fruits and vegetables deeply processing. process of fruits and vegetables [12], are abundant and widely distributed in various kinds of plants. Existing research demonstrates that PPO mainly exists in the cytoplasmic membrane and cell walls, and phenols usually accumulate in vacuoles [13]. Fruit tissue structure and regionalization of the cell space are damaged by fresh-cut operations, destroying partitions between PPO and substrate polyphenols and allowing contact between enzymes and substrates for catalysis by PPO of the transformation of contact the transformation of, phenolic compounds into quinone compounds [14]. Melanins are accumulated through secondary enzyme reactions, inducing the enzymatic browning reaction [15–18]. Liu et al. [19] studied the reaction mechanism of enzymatic browning during potato processing, and analyzed the correlation between substrates and browning. Their results showed that phenolic compounds are closely related to browning, and chlorogenic acid is an important substrate leading to potato enzymatic browning. The phenolic compounds identified in banana peels in recent years were mainly dopamine, followed by chlorogenic acid and coumarin, with dopaminerase oxidation being the main factor for banana browning [20]. Chlorogenic acid and epicatechin are the phenolic compounds with the highest contents in apple fruits [21], while the substrates in mango are mainly coffeic acid and ferulic acid [22]. The substrates for litchi peel browning belong to the collated catechenol compounds, which can rapidly interact with PPO to form browning products [23]. Free polyphenols are the main substrates in the browning reaction of longan peels, and the effect of anthocyanins in the browning reaction is not obvious [24]. The content of polyphenols reflects the antioxidant capacity of fruits and vegetables. Research results of Liu et al. [25] showed that peach phenols are chrologenic acid, neo-chlorogenic acid, protocatechuic acid. Mishra et al. [26] also showed that browning of eggplant was related to the content increased of polyphenols. In this study, chlorogenic acid, dopamine, caffeic acid, cinnamic acid and vanillin were found in eggplant fruits, and the metabolite analysis showed that the content of chlorogenic acid, dopamine, caffeic acid and cinnamic acid was increased after peeling; the content of chlorogenic acid accumulated at an extremely significant level ($p = 0.0025$), but the content of flavonoids such as soybean vanillin did not change significantly, suggesting that the main substrate of enzymatic browning in eggplant is chlorogenic acid.

PPO is involved in the tyrosine metabolism pathway. Tyrosine can produce L-dopamine under the action of PPO, which is converted to dopamine quinone, leading to the occurrence of browning [27]. In this study, the tyrosine metabolism pathway was the common metabolic pathway showing significant differences between the 3min/CK and 5min/CK comparison groups. It is worth noting that the vanillylmandelic acid content decreased at 3 min after peeling, but was rising again at 5 min, although it was still lower than that in the CK group. This is because after the eggplant was peeled, vanillylmandelic acid was oxidized by PPO through tyrosine metabolism and converted into quinones, and finally polymerized into brown substances, leading to browning.

In addition, phenylalanine ammonialyase (PAL) plays a momentous role in regulating the production of phenolic substances in the phenylalanine pathway and is an important enzyme regulating browning [28]. L-phenylalanine rooted in the Shikimate pathway generates trans-cinnamic acid via PAL ammonia solution reaction. The trans-cinnamic acid then enters into phenylpropanol metabolism and generates intermediates including coumaric acid, ferulic acid and mustard acid that can be further converted to coumarin and chlorogenic acid, and also can form CoA esters. Finally,

these are converted to flavonoids, lignin, alkaloids and other secondary metabolites [29–30]. In this study, we detected the phenylpropanol metabolism pathway in the 3min/CK comparison, with the accumulation of L-tryptophan and chlorogenic acid up-regulated. The biosynthesis pathway for flavonoids was found in the 3min/CK and 5min/CK comparisons, where the participation of quercetin was down-regulated. Mechanical injury by peeling can significantly increase PAL activity, and phenols are changed by the phenylpropanol metabolism pathway and flavonoids biosynthesis pathway. At the same time, the membrane system is destructed, and the regional distribution of enzymes and substrates is disrupted, allowing phenols to be catalyzed by PPO under action of reactive oxygen species (ROS), eventually generating brown substances.

Fruits contain ROS, including super oxygen anion free radical (O^{2-}), hydrogen peroxide (H_2O_2) and hydroxyl free radical (-OH). Mechanical damage when fruits and vegetables are cut, destroys the plant ROS metabolism balance. A large increase of ROS may be lead to the cell membrane lipid peroxidation and destroy the integrity of the cell, which caused the cell aging and death [31–33]. In this study, glutathione metabolism was found in all three groups, and the content of L-glutamate involved in this pathway increased, while the content of threonine decreased. Therefore, we hypothesized that in exist of H_2O_2, phenols and flavonoids are catalyzed by POD after eggplant is peeled and aggregate into brown substances causing fruit browning. Alternatively, glutathione in fruits and vegetables is oxidized, through glutathione metabolism, and the content of L-glutamic acid is increased while the content of threonine is decreased, which accelerating aging and affecting the flavor and nutrition of fruits and vegetables.

Furthermore, the analysis of metabolites gave a comprehensive overview of the active pathways after eggplant is peeled. Glycosylphosphatidyl-inositol anchored protein(GPI), is an integral protein involved in the endoplasmic reticulum and plasma membranes on GPI [34–35]. Like all fatty acids, Linoleic acid can be perceived as a material source of cellular energy [36]. Linoleic acid is a part of membrane phospholipid, which is an essential structural part to sustain a particular level of membrane fluidity. And in vivo it can be esterified to come into being lipids such as cholesterol esters and triacylglycerols [37]. Moreover, when it is released from membrane phospholipids, can be enzymatically oxidized into all kinds of derivatives participate in cell metabolism and signal transduction [38]. In addition, we also found that the content of some alkaloids, such as L(-)-Nicotine, enoxacin and neocnidilide, were decreased as peeled time increased, through tropane, piperidine and pyridine alkaloid biosynthesis. The pentose phosphate pathway provides substrates for essential biosynthetic pathways [39]. In this study, linoleic acid metabolism, the glycosylphosphati-dylinositol (GPI)-anchor, Tropane, piperidine and pyridine alkaloid biosynthesis, and pentose phosphate pathways at the three different treatment stages after peeling were significantly different. Therefore, we hypothesize that these metabolic pathways may play an important role in the browning of fruits and vegetables.

Conclusions

The present investigation clearly demonstrated that metabolomics analysis is a good tool for explaining the browning mechanism of eggplant by detecting changes in the expression of metabolites and differences in metabolic pathways after peeling. There were pronounced changes in metabolites in eggplant for at 3 min and 5 min after peeling. Several hundred differential metabolites were identified, including lipids, phenols, sugars and fatty acids etc. The metabolite contents changed dynamically as the peeled time increased. Furthermore, by analyzing the KEGG pathway of these differential metabolites, we found that some metabolic pathways were perturbed after peeling, such as linoleic acid metabolism, glutathione metabolism, pentose phosphate pathway, tropane, piperidine and pyridine alkaloid biosynthesis, phenylpropanol metabolism and tyrosine metabolism, and these showed significant differences over time. The identified metabolites and metabolic pathways may have specific effects on various aspects of fruit and vegetable browning. We established an untargeted metabolomics method based on LC-MS technology to explain the mechanism of eggplant browning, which provides new ideas and perspectives for understanding fruit browning in the future.

Methods

Plant material

Eggplant cultivar ‘Huqie 5’ is a breeding line produced by our lab at the Shanghai Academy of Agricultural Sciences, Shanghai, China. Pulp of peeled eggplant after 0, 3 and 5 min was taken as experimental materials.

Instruments and chemicals

Vortex oscillator (TYXH-I, Shanghai Hanno Instrument Co., Ltd); Automatic sample rapid grinding machine (JXFSTPRP–24/32, Shanghai Jingxin Industrial Development Co., Ltd); Table top high-speed refrigerated centrifuge (TGL–16MS, Shanghai Lu Xiangyi Centrifuge Instrument Co., Ltd); Ultrasonic cleaning machine (SB–5200DT, Ningbo Xinzhi Biotechnology Co., Ltd); Ultra high performance liquid chromatography (ACQUITY UPLC, Waters); Chromatographic column(ACQUITY UPLC BEH C18 (100 mm ×2.1 mm, 1.7 μm), Waters); High-resolution mass spectrometry (AB Triple TOF 5600, AB Sciex). We selected methanol, formic acid, acetonitrile, water from CNW Technologies GmbH and l–2-chlorophenylalanine from Shanghai hengchuang biotechnology co., LTD. Note: all chemical reagents and solvents are analytically pure or chromatographic grade.

Sample preparation

Preparation of samples for metabolites extraction was conducted by transferring 80 mg of lyophilized sample a 1.5 mL Ep tube. The internal standard was 2-chlorine-l-phenylalanine (20 μL, 0.3 mg/mL soluble in methanol). Each sample was added with a methanol and water mixture (7:3,v/v, 1000 μL) and placed at −20°C for 2 minutes. The sample was ground at 60 Hz for 2 min, followed by 4°C ultrasound for 30 min after brief eddy current, placed at −20°C for 20 min and was centrifuged at 1000×g and 4°C for 15 min. The supernatant of 200 μL in per tube was gathered by a crystal syringe, filtered through a 0.22 μm microfilter and transferred to an automatic sampling bottle for LC-MS analysis. The vials were stored at −80℃ until they were used for LC-MS analysis. QC samples were made from a mixture of each of the samples; the volume of each QC sample was the same as that of the sample. Before use, all extraction reagents should be precooled at −20℃.

LC-MS analysis

The analytical instrument of this experiment is The UHPLC system that is composed of liquid-mass coupling system consisted of AB Sciex Triple TOF 5600 high resolution mass spectrometer. It was appiled to analyze metabolic profiles in both TIC+ and TIC- modes.

Chromatographic conditions were as follows: Chromatographic column: ACQUITY UPLC BEH C18 (100 mm × 2.1 mm, 1.7 m); column temperature: 45℃; mobile phase: A—water (containing 0.1% formic acid), B—acetonitrile (containing 0.1% formic acid); flow rate: 0.4 mL/min; injection volume: 5 μL. The elution gradient is shown in Table 3. Mass spectrometry conditions are shown in Table 4. In addition, in order to assess the repeatability of the whole analysis process, we added one QC sample per 8 analysis samples.

Data preprocessing and statistical analyses

The original data were disposed using progenesis QI made in Waters Corporation from Milford of USA. Then, we constructed a data matrix that was inputed into XCMS software (version 14.0, Umetrics, Umeå, Sweden), in which PCA, PLS-DA and OPLS-DA were executed. The 95% confidence interval that defines the change of the model is represented by the Hotelling’s T2 region. It is represented as an ellipse in the rating diagram of the model. The reliability of the model is illuminated by the terms R2X or R2Y and Q2. R2X represents the cumulative interpretation rate of the multivariate

statistical analysis modeling. R2Y represents the cumulative interpretation rate in the Y-axis model. Therefore, R2X or R2Y indicate the goodness of fit. R2 and Q2 are the parameters of response sequencing test, used to measure whether the model is overfitted, so as to represent predictability, which can be calculated through the cross-validation process. To prevent overfitting of the model, seven fold cross-validation and 200 RPT were applied to evaluate the quality of the model.

Identification of differential metabolites

The difference metabolites between groups were screened out using the methods of multi-dimensional analysis and one-dimensional analysis. The screening criteria were VIP >1 for the first principal component of the OPLS-DA model, and $p < 0.05$ for the Student's t-test, where the variation multiple was the ratio of the average metabolites in the two groups. Metabolites were described using progenesis QI (Waters Corporation, Milford, USA) metabolic data software based on public databases (http://www.hmdb.ca/; http://www.lipidmaps.org/) and a self-built database. Furthermore, the identified metabolites were classified to different compounds using the Human Metabolome Database (HMDB, http://www.hmdb.ca/).

KEGG pathway analysis

These differential metabolites were mapped onto the KEGG database, and metabolic pathways were analyzed based on KEGG (http://www.genome.jp/KEGG/pathway.html) pathway analysis.

Declarations

Abbreviations

LC-MS: Liquid Chromatography-Mass Spectrometry; TIC+: The positive Ion Current; TIC-: The negative Ion Current; PCA: Principal Component Analysis; PLS-DA: Partial Least Squares Discriminant Analysis; OPLS-DA: Orthogonal Partial Least Squares Discriminant Analysis; VIP: Variable Importance in the Projection; PPO: Polyphenol Oxidase; PAL: Phenylalnine Ammonialyase; POD: Peroxidase; RPT: Response Permutation Tests; QC: Quality control; KEGG: Kyoto Encyclopedia of Genes and Genomes; HMDB: Human Metabolome Database.

Ethics approval and consent to participate

Not applicable.

Consent to publication

Not applicable.

Availability of data and materials

The data charts supporting the results and conclusions are included in the article and additional files.

Competing interests

The authors declare that they have no competing interests.

Funding

This work was supported by the China Agriculture Research System (Grant No. CARS-25) and Shanghai Academy of Agricultural Sciences Outstanding Team Construction Project [Agricultural Science Branch 2017(b06)].

Authors' contributions

DZ and XW put forward and designed the research, ZZ and AZ carried out the preparation of the experiment. SZ and JS performed the treatment of test materials. XL analyzed the data and wrote the manuscript. All authors read and approved the final manuscript.

Acknowledgements

Not applicable.

Authors' Information

[a]Shanghai Ocean University, Shanghai 201306, China

[b]Horticultural Research Institute, Shanghai Academy of Agricultural Sciences, Shanghai 201403, China

[c]Shanghai Key Laboratory of Protected Horticultural Technology, Shanghai 201403, China

References

1. Nicholson J K, Lindon J C, Holmes E. 'Metabonomics': understanding the metabolic responses of living systems to pathophysiological stimuli via multivariate statistical analysis of biological NMR spectroscopic data. Xenobiotica. 1999;29:1181-9.
2. Fiehn O. Metabolomics - the link between genotypes and phenotypes. Plant Mol Biol. 2002;48:155-71.
3. Wang QZ, Wu CY, Chen T, Chen X, Zhao XM. Integrating metabolomics into a systems biology framework to exploit metabolic complexity: strategies and applications in microorganisms. Appl Microbiol Biotechnol. 2006;70:151-161.
4. Dethloff F, Erban A, Orf I, Alpers J, Fehrle I, Beine-Golovchuk O, et al. Profiling methods to identify cold-regulated primary metabolites using gas chromatography coupled to mass spectrometry. Methods Mol Biol. 2014;1166:171-97.
5. Hong J, Yang L, Zhang D, Shi J. Plant Metabolomics: An Indispensable System Biology Tool for Plant Science. Int J Mol Sci. 2016;17: pii: E767.
6. Sheflin AM, Chiniquy D, Yuan C, Goren E, Kumar I, Braud M, et al. Metabolomics of sorghum roots during nitrogen stress reveals compromised metabolic capacity for salicylic acid biosynthesis. Plant Direct. 2019;3:e00122.
7. Fragallah SADA, Wang P, Li N, Chen Y, Lin S. Metabolomic Analysis of Pollen Grains with Different Germination Abilities from Two Clones of Chinese Fir (Cunninghamia lanceolata (Lamb) Hook). Molecules. 2018;23:3162.
8. Du B, Kruse J, Winkler JB, Alfarray S, Schnitzler JP, Ache P, et al. Climate and development modulate the metabolome and anti-oxidative system of date palm leaves. J Exp Bot. 2019;pii:erz361.
9. Dinesh K S, Prashant K. Visiting eggplant from a biotechnological perspective: A review. Sci Hortic. 2019;253:327-340.
10. Bhushan B, Kumar S, Mahawar MK, Jalgaonkar K, Dukare AS, Bibwe B, et al. Nullifying phosphatidic acid effect and controlling phospholipase D associated browning in litchi pericarp through combinatorial application of hexanal and inositol. Sci Rep. 2019;9:2402.
11. Mishra B, Gautam S, Sharma A. Browning of fresh-cut eggplant: Impact of cutting and storage. Postharvest Biol and Technol. 2012;67:44-51.
12. Vanden AC, Raes K, Sampers L. Effect of mild heat treatment on browning-related parameters in fresh-cut Iceberg lettuce. Food Biochem. 2019;43:e12906.

13. Qi J, Li GQ, Dong Z, Zhou W. Transformation of tobacco plants by Yali PPO-GFP fusion gene and observation of subcellular localization. Am J Transl Res. 2016;8:698-704.
14. Taranto F, Pasqualone A, Mangini G, Tripodi P, Miazzi MM, Pavan S, et al. Polyphenol Oxidases in Crops: Biochemical, Physiological and Genetic Aspects. Int J Mol Sci. 2017;18:pii: E377.
15. Amaki K, Saito E, Taniquchi K, Joshita K, Murata M. Role of chlorogenic acid quinone and interaction of chlorogenic acid quinone and catechins in the enzymatic browning of apple. Biosci Biotechnol Biochemi. 2011;75:829-832.
16. Lin YF, Lin HT, Lin YX, Zhang S, Chen YH, Jiang XJ. The roles of metabolism of membrane lipids and phenolics in hydrogen peroxide-induced pericarp browning of harvested longan fruit. Postharvest Biol Technol. 2016;111:53-61.
17. Sheng L, Zhou X, Liu ZY, Wang JW, Zhou Q, Wang L, et al. Changed activities of enzymes crucial to membrane lipid metabolism accompany pericarp browning in 'Nanguo' pears during refrigeration and subsequent shelf life at room temperature. Postharvest Biol Technol. 2016;117:1-8.
18. Wang Y, Jiang G, Li M, Lv M, Zhou X, Zhou Q, et al. Effect of low temperature storage on energy and lipid metabolisms accompanying peel browning of 'Nanguo' pears during shelf life. Postharvest Biol Technol. 2018;139:75-81.
19. Liu X, Yang Q, Lu Y, Li Y, Li T, Zhou B, Qiao L. Effect of purslane (*Portulaca oleracea*) extract on anti-browning of fresh-cut potato slices during storage. Food Chem. 2019;283:445-53.
20. Escalante-Minakata P, Ibarra-Junquera V, Ornelas-Paz JJ, García-Ibáñez V, Virgen-Ortíz JJ, González-Potes A, et al. Comparative study of the banana pulp browning process of 'Giant Dwarf' and FHIA-23 during fruit ripening based on image analysis and the polyphenol oxidase and peroxidase biochemical properties. 2018;8:30.
21. Park SY, Kang TM, Kim MJ, Kim MJ. Enzymatic browning reaction of apple juices prepared using a blender and a low-speed masticating household juicer. Biosci Biotechnol Biochem. 2018;82:2000-6.
22. Prasad K, Sharma RR, Srivastav M. Postharvest treatment of antioxidant reduces lenticel browning and improves cosmetic appeal of mango (*Mangifera indica*) fruits without impairing quality. J Food Sci Technol. 2016;53:2995-3001.
23. Ali S, Khan AS, Malik AU, Anjum MA, Nawaz A, Shah HMS. Modified atmosphere packaging delays enzymatic browning and maintains quality of harvested litchi fruit during low temperature storage. Sci Hortic. 2019;254:14-20.
24. Wang H, Chen YH, Sun JZ, Lin YF, Lin YX, Lin M, et al. The Changes in Metabolisms of Membrane Lipids and Phenolics Induced by Phomopsis longanae Chi Infection in Association with Pericarp Browning and Disease Occurrence of Postharvest Longan Fruit. J Agric Food Chem. 2018;66:12794-804.
25. Liu H, Jiang WB, Cao JK, Li YC. Effect of chilling temperatures on physiological properties, phenolic metabolism and antioxidant level accompanying pulp browning of peach during cold storage. Sci Hortic. 2019;255:175-82.
26. Mishra BB, Gautam S, Sharma A. Free phenolics and polyphenol oxidase (PPO): The factors affecting post-cut browning in eggplant (*Solanum melongena*) . Food Chemistry. 2013;139:105-14.
27. Yingsanga P, Srilaong V, Kanlayanarat S, Noichinda S, McGlasson WB. Relationship between browning and related enzymes (PAL, PPO, and POD) in rambutan fruit (*Nephelium lappaceum*) cvs. Rongrien and See-Chompoo. Postarvest Biol Technol. 2008;50:164-8.
28. Tomas-Barberan FA, Espin JC. Phenolic compounds and related enzymes as determinants of quality in fruits and vegetables. J Sci Food Agric. 2001;81:853-76.
29. Bharat B, Ajay P, Rajesh N, Meena VS, Sharma PC, Singh J. Combinatorial approaches for controlling pericarp browning in Litchi (Litchi chinensis) fruit. J Food Sci Technol. 2015;52:5418-26.
30. Liu X, Lu Y, Yang Q, Yang HY, Li Y, Zhou BY, et al. Cod peptides inhibit browning in fresh-cut potato slices: A potential anti-browning agent of random peptides for regulating food properties. Postharvest Biol Technol.

2018;146:36-42.

31. Wang H, Chen Y, Lin H, Sun J, Lin Y, Lin M. Phomopsis longanae Chi-Induced Change in ROS Metabolism and Its Relation to Pericarp Browning and Disease Development of Harvested Longan Fruit. Front Microbiol. 2018;9:2466.
32. Sun J, Lin H, Zhang S, Lin Y, Wang H, Lin M, et al. The roles of ROS production-scavenging system in Lasiodiplodia theobromae (Pat.) Griff. & Maubl.-induced pericarp browning and disease development of harvested longan fruit. Food Chem. 2018;247:16-22.
33. Li T, Shi D, Wu Q, et al. Sodium para-aminosalicylate delays pericarp browning of litchi fruit by inhibiting ROS-mediated senescence during postharvest storage[J]. Food Chem, 2019, 278: 552-559.
34. Gao J, Guo Z. Recent progress in the synthesis of GPIs and GPI-anchored proteins. Sci Sinica Chimica. 2013;43:964-83.
35. Kinoshita T, Fujita M. Thematic review series: Glycosylphosphatidylinositol (GPI) anchors: Biochemistry and cell biology: Biosynthesis of GPI-anchored proteins: Special emphasis on GPI lipid remodeling. Lipid Res. 2016;57:6.
36. Whelan J, Fritsche K. Linoleic Acid. Adv Nutr. 2013;4:311-2.
37. Xia J, Zheng M, Li L, Hou X, Zeng W. Conjugated linoleic acid improves glucose and lipid metabolism in diabetic mice. Nan Fang Yi Ke Da Xue Xue Bao. 2019;39:740-6.
38. Mika A, Czumaj A, Stepnowski P, Macaluso F, Spinoso G, Barone R, et al. Exercise and Conjugated Linoleic Acid Supplementation Induce Changes in the Composition of Liver Fatty Acids. Front Physiol. 2019;10:602.
39. Andriotis VME, Smith AM. The plastidial pentose phosphate pathway is essential for postglobular embryo development in Arabidopsis. Proc Natl Acad Sci. 2019;116:15297-306.

Additional Files

Additional file 1: Table S1 Data matrix

Additional file 2: Table S2 The differential metabolites among the three comparison groups

Additional file 3: Table S3 The 119 common differential metabolites from the 3min/CK and 5min/CK groups were further divided into three sorts represented by A, B and C

Additional file 4: Table S4 The raw data in fig. 6

Tables

No.	Model	Type	A	N	R2X(cum)	R2Y(cum)	Q2(cum)	R2	Q2
All	M1	PCA-X	6	32	0.651		0.356		
5min/CK	M2	PCA-X	3	16	0.62		0.416		
5min/CK	M3	PLS-DA	2	16	0.502	0.989	0.955		
5min/CK	M4	OPLS-DA	1+2+0	16	0.64	0.998	0.987	0.642	-0.849
3min/CK	M5	PCA-X	4	16	0.612		0.106		
3min/CK	M6	PLS-DA	3	16	0.479	0.995	0.889		
3min/CK	M7	OPLS-DA	1+3+0	16	0.595	0.998	0.925	0.795	-0.88
3min/5min	M8	PCA-X	4	16	0.662		0.321		
3min/5min	M9	PLS-DA	3	16	0.562	0.995	0.956		
3min/5min	M10	OPLS-DA	1+1+0	16	0.466	0.985	0.943	0.522	-0.741

Table 1 The parameters for the assessment of these models.

	Benzenoids	Fatty acids	lipids	Organic acids	Organoheterocyclic compounds	Carbohydrates	Amines	Hydrocarbons
A	1	13	22	6	9	17	0	0
B	3	14	13	3	4	1	1	1
C	1	1	7	2	0	0	0	0

Table 2 Classification of metabolites

Time(min)	A%	B%
0	95	5
2	80	20
4	75	25
9	40	60
14	0	100
18	0	100
18.1	95	5
19.5	95	5

Table 3 Elution gradient

parameters	positive	negitive
Nebulizer Gas (GS1, PSI)	40	40
Auxiliary Gas (GS2, PSI)	40	40
Curtain Gas (CUR, PSI)	35	35
Ion Source Temperature (°C)	550	550
Ion Spray Voltage (V)	5500	4500
Declustering Potential (DP ,V)	100	-100
Mass Scan Range (TOF MS scan)	70-1000	70-1000
Collision Energy (TOF MS scan, eV)	10	-10
Mass Scan Range (Product Ion scan)	50-1000	50-1000
Collision Energy (Product Ion scan,eV)	30	30
Interface Heater Temperature (°C)	550	600

Table 4 MS parameters

Figures

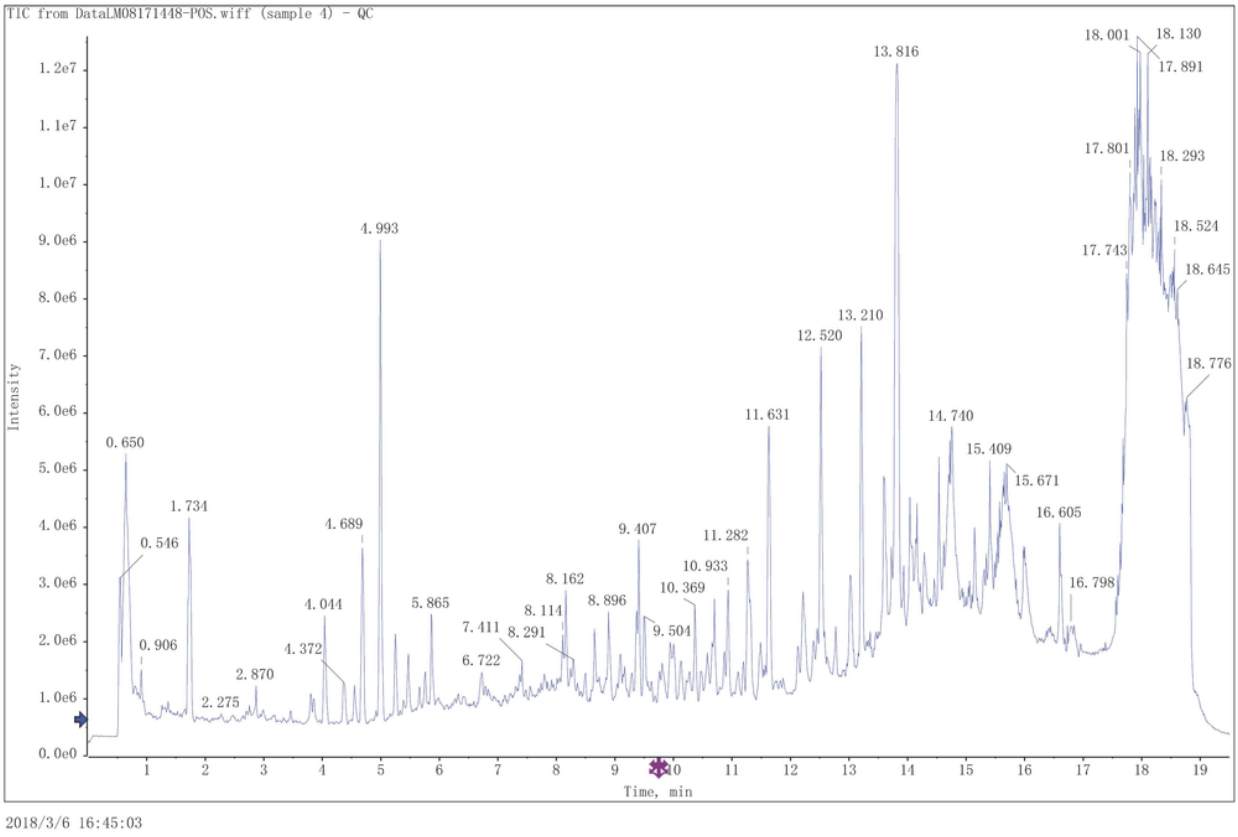

Figure 1

The TIC+ total ion flow diagram of QC

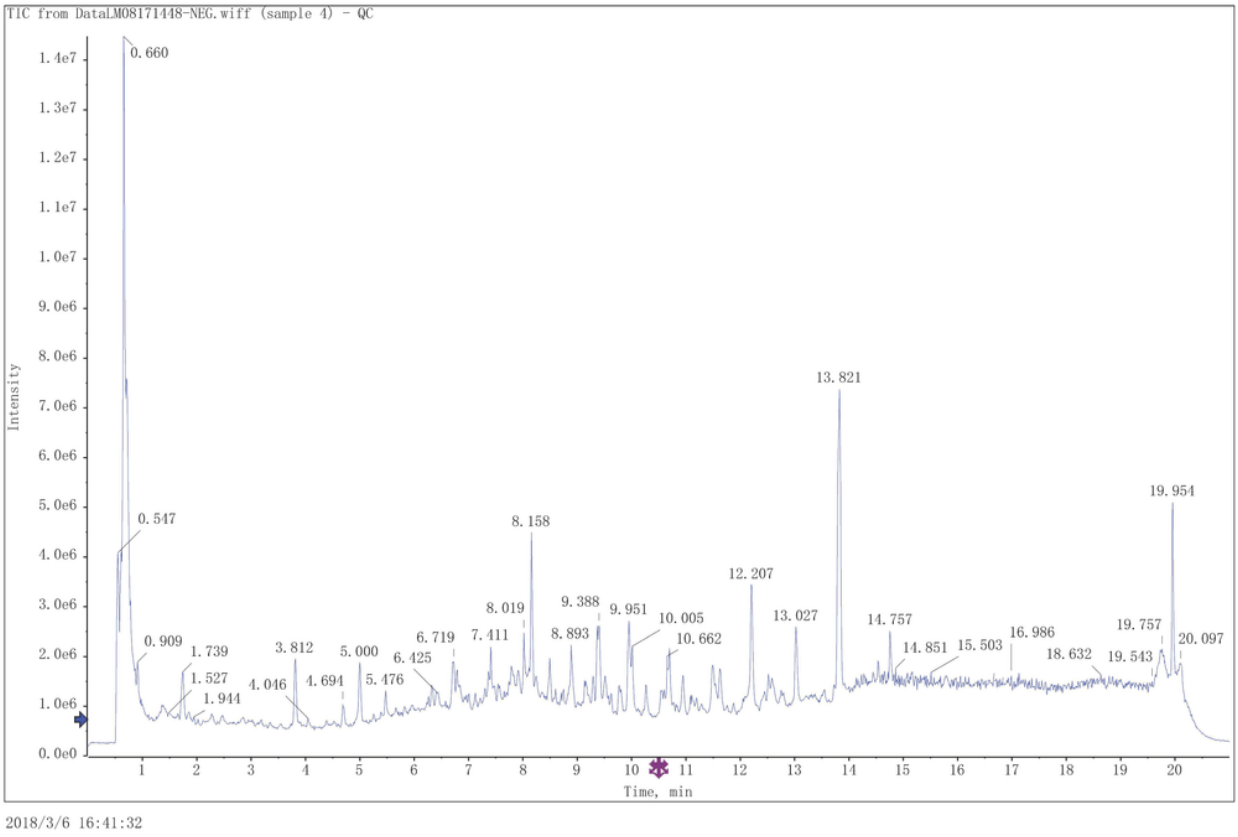

Figure 2

The TIC- total ion flow diagram of QC

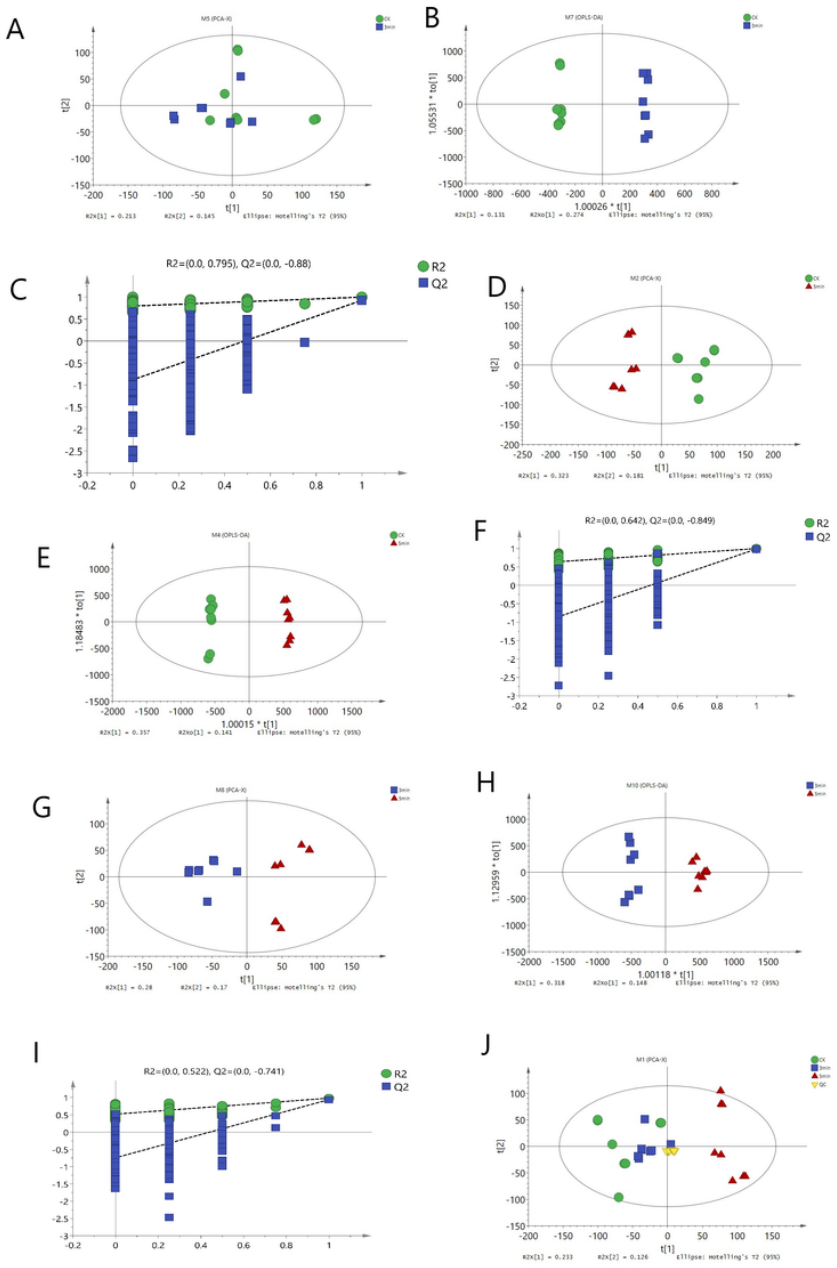

Figure 3

Scores of PCA, PLS-DA, OPLS-DA and validation plots of OPLS-DA for 3min/CK、5min/CK and 3min/5min. (a) PLS-DA for 3min/CK. (b) OPLS-DA for 3min/CK. (c) validation plots of OPLS-DA for 3min/CK. (d) PLS-DA for 5min/CK. (e) OPLS-DA for 5min/CK. (f) Validation plots of OPLS-DA for 5min/CK. (g) PLS-DA for 3min/5min. (h) OPLS-DA for 3min/5min. (i) Validation plots of OPLS-DA for 3min/5min. (j) Score scatter plots of PCA for all comparative groups

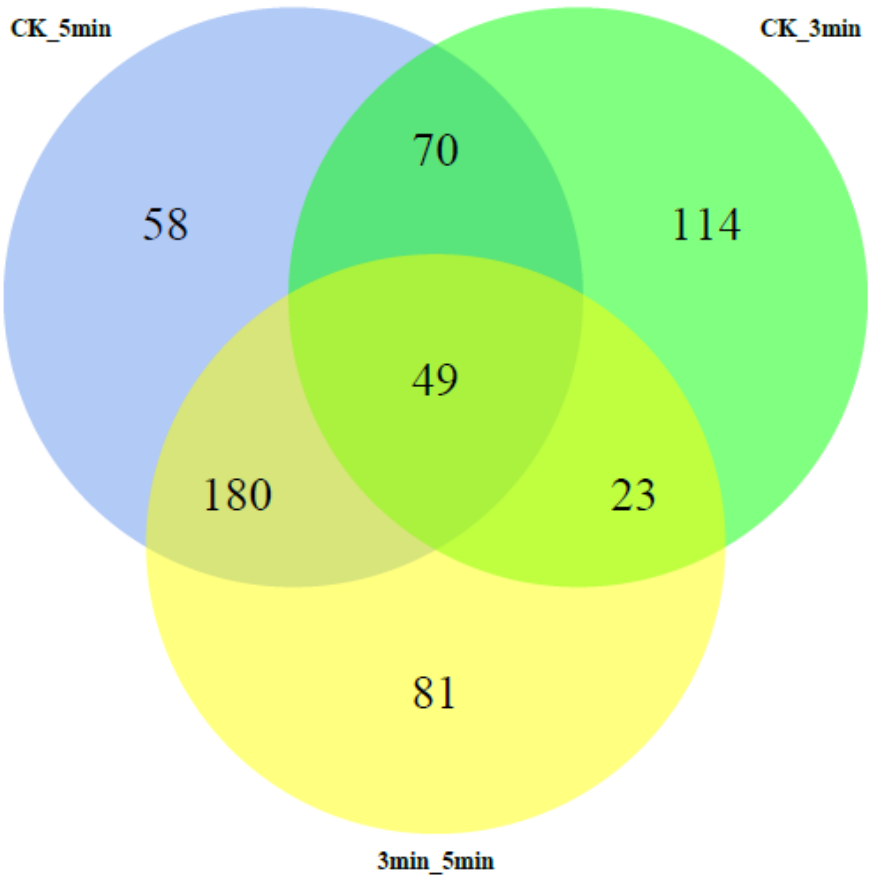

Figure 4

Venn diagram of the differential metabolites among three comparative groups

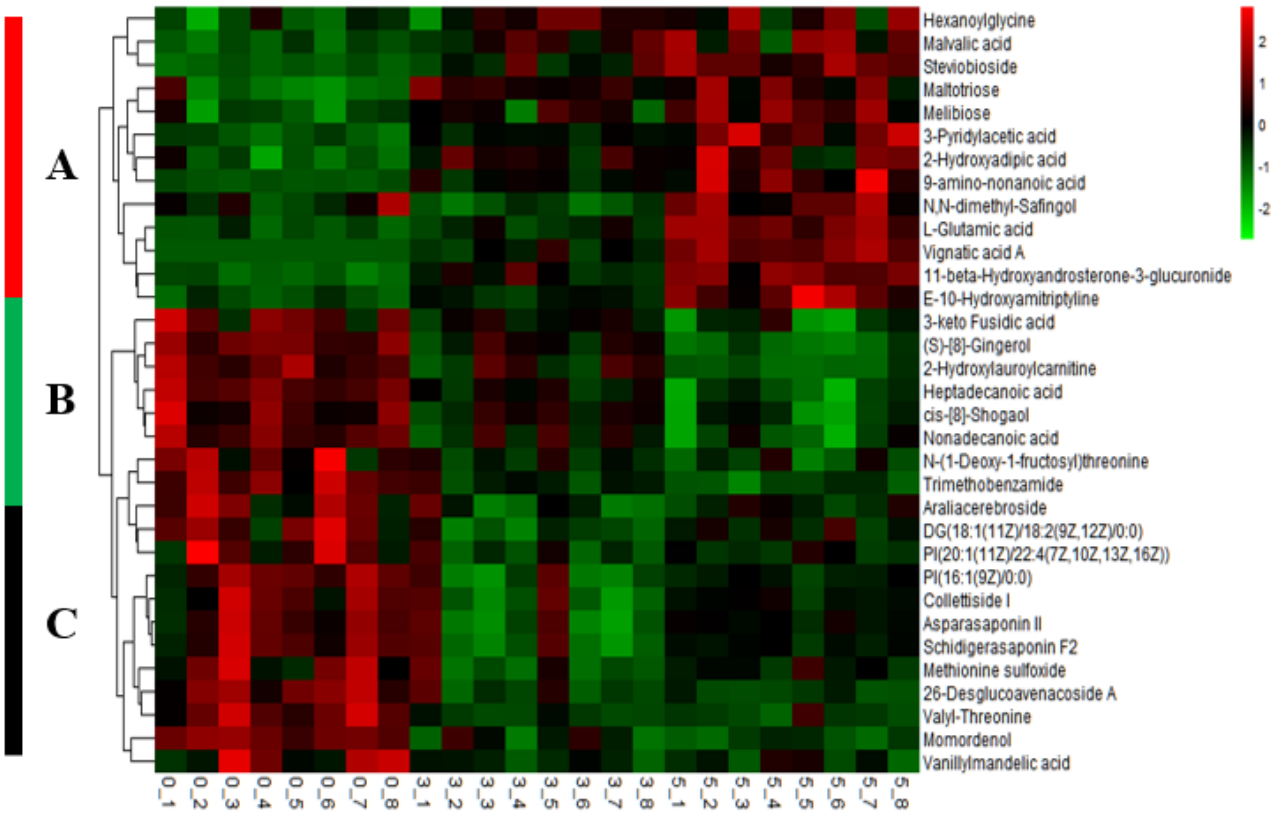

Figure 5

Heatmap shows the differences in the expression levels of metabolites

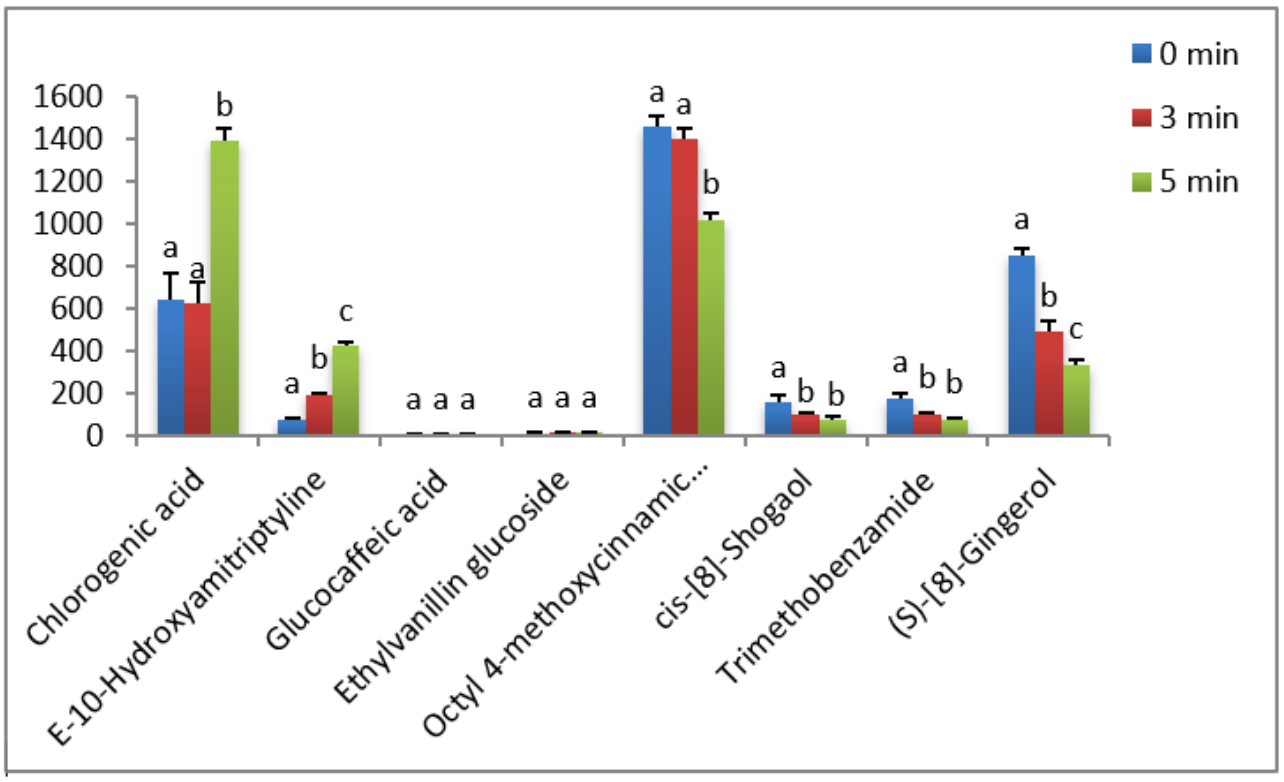

Figure 6

The differences in phenols content at the three treatment stages

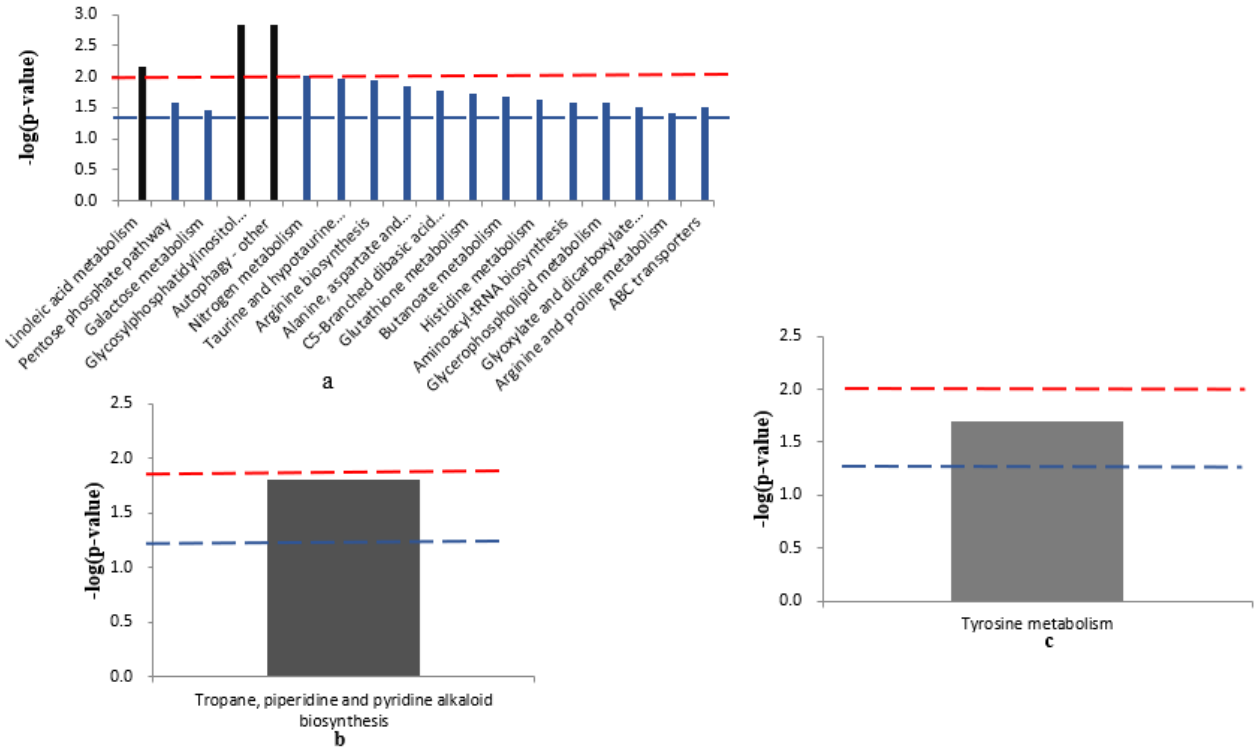

Figure 7

The differential metabolic pathways (a) The differential metabolic pathways that be enriched by the metabolites of category (A). (b) The differential metabolic pathway that be enriched by the metabolites of category (B). (c) The differential metabolic pathway that be enriched by the metabolites of category (C). The red line indicates that the p-value=0.01, and the blue line indicates that the p-value=0.05. When the top of a column is higher than the blue or red line, the metabolic pathway shows significant differences.

Supplementary Files

This is a list of supplementary files associated with this preprint. Click to download.

- Additionalfile2TableS2.xlsx
- Additionalfile1TableS1.xlsx
- Additionalfile3TableS3.xlsx
- Additionalfile4TableS4.xlsx